



# Comparison of distribution and toxicity following repeated oral dosing of different vanadium oxide nanoparticles in mice



Eun-Jung Park <sup>a,\*1</sup>, Gwang-Hee Lee <sup>b,1</sup>, Cheolho Yoon <sup>c</sup>, Dong-Wan Kim <sup>b,\*\*</sup>

<sup>a</sup> Myunggok Eye Research Institute, Konyang University, Daejeon 302-718, South Korea

<sup>b</sup> School of Civil, Environmental, and Architectural Engineering, Korea University, Seoul 136-713, South Korea

<sup>c</sup> Seoul Center, Korea Basic Science Institute, Seoul 126-16, South Korea

## ARTICLE INFO

### Article history:

Received 1 April 2016

Received in revised form

11 May 2016

Accepted 19 May 2016

Available online 9 June 2016

### Keywords:

Vanadium oxide nanoparticles

Toxicity

Distribution

Redox reaction

Ion homeostasis

## ABSTRACT

Vanadium is an important ultra-trace element derived from fuel product combustion. With the development of nanotechnology, vanadium oxide nanoparticles (VO NPs) have been considered for application in various fields, thus the possibility of release into the environment and human exposure is also increasing. Considering that verification of bioaccumulation and relevant biological responses are essential for safe application of products, in this study, we aimed to identify the physicochemical properties that determine their health effects by comparing the biological effects and tissue distribution of different types of VO NPs in mice. For this, we prepared five types of VO NPs, commercial (C)-VO<sub>2</sub> and -V<sub>2</sub>O<sub>5</sub> NPs and synthetic (S)-VO<sub>2</sub>, -V<sub>2</sub>O<sub>3</sub>, and -V<sub>2</sub>O<sub>5</sub> NPs. While the hydrodynamic diameter of the two types of C-VO NPs was irregular and impossible to measure, those of the three types of S-VO NPs was in the range of 125–170 nm. The S- and C-V<sub>2</sub>O<sub>5</sub> NPs showed higher dissolution rates compared to other VO NPs. We orally dosed the five types of VO NPs (70 and 210 µg/mouse, approximately 2 and 6 mg/kg) to mice for 28 days and compared their biodistribution and toxic effects. We found that S-V<sub>2</sub>O<sub>5</sub> and S-V<sub>2</sub>O<sub>3</sub> NPs more accumulated in tissues compared to other three types of VO NPs, and the accumulated level was in order of heart > liver > kidney > spleen. Additionally, tissue levels of redox reaction-related elements and electrolytes (Na<sup>+</sup>, K<sup>+</sup>, and Ca<sup>2+</sup>) were most clearly altered in the heart of treated mice. Notably, all S- and C-VO NPs decreased the number of WBCs at the higher dose, while total protein and albumin levels were reduced at the higher dose of S-V<sub>2</sub>O<sub>5</sub> and S-V<sub>2</sub>O<sub>3</sub> NPs. Taken together, we conclude that the biodistribution and toxic effects of VO NPs depend on their dissolution rates and size (surface area). Additionally, we suggest that further studies are needed to clarify effects of VO NPs on functions of the heart and the immune system.

© 2016 Elsevier Inc. All rights reserved.

## 1. Introduction

Nanotechnology is defined as the manipulation of matter that has at least one size dimension as small as 1–100 nm. Unusual physical, chemical, and biological properties can emerge in materials at this nanoscale, and these can differ in important ways from the corresponding properties of bulk materials and single atoms or molecules (National Nanotechnology Initiative, 2014). Given the rapid development of nanotechnology, governments have invested billions of dollars to create new materials and devices with applications in diverse fields, such as in medicine,

electronics, biomaterials, energy production, and consumer products (Allianz AG and the Organisation for Economic Co-operation and Development, 2005). On the other hand, toxicologists have continuously raised concerns about the potential for adverse health effects that could be associated with increased human and environmental exposure to nanomaterials.

Vanadium is an important ultra-trace element derived from fuel product combustion, so it is widely distributed in nature (Bell et al., 2014; Imtiaz et al., 2015). Additionally, it has received special and long-standing attention in the pharmacological area including the regulation of intracellular signaling, as a cofactor of enzymes essential in energy metabolism, as an alternative therapeutic agent for the treatment of diabetes mellitus, and as a potential cancer chemo-preventative agent owing to its unique biological function (Basu et al., 2014; Bishayee and Chatterjee, 1993; Thompson, 1999). Vanadium pentoxide (V<sub>2</sub>O<sub>5</sub>) has been also widely used as a catalyst for ferrovanadium and sulfuric acid production in industry owing to its high oxidation state (Reference). Moreover, engineers

\* Corresponding author at: Myunggok Eye Research Institute, Konyang University, Daejeon 302-718, South Korea.

\*\* Corresponding author at: School of Civil, Environmental, and Architectural Engineering, Korea University, Seoul 136-713, South Korea.

E-mail addresses: [pejtoxic@hanmail.net](mailto:pejtoxic@hanmail.net) (E.-J. Park),

[dkw1@korea.ac.kr](mailto:dkw1@korea.ac.kr) (D.-W. Kim).

<sup>1</sup> These authors contributed equally to this work.

have recently been studying vanadium oxide (VO) nanoparticles (NPs) as a material for potential use in electrochemistry, catalysis, and energy storage (Langeroodi, 2012; Ng et al., 2009; Zhu et al., 2015). On the other hand, many researchers have suggested that VOs are not suitable for application in the pharmaceutical area due to the possibility of strong biological side effects (Domingo, 1996; Reul et al., 1999) and that their release into the environment should be rigorously regulated (Basu et al., 2014; Beyersmann and Hartwig, 2008; Keil et al., 2016; Kim et al., 2003; Magari et al., 2002). For example, although symptoms such as hyperglycemia, hyperphagia, and polydipsia were significantly ameliorated by vanadium treatment in diabetic rats, side effects such as tissue accumulation, decreased weight gain, and death were observed in all vanadium treated-rats. (Domingo et al., 1991). Furthermore, inhalation of V<sub>2</sub>O<sub>5</sub> has been shown to impair immune cell function and increase the risk of cancer (Cohen et al., 2007; Ehrlich et al., 2008; Pinon-Zarate et al., 2008).

The physicochemical properties of NPs, especially shape and size, play a central role in determining their toxicity, therefore should be extensively evaluated in defining regulatory guidelines. Accumulating evidence also shows that the toxicity of VO NPs can be influenced by oxidation state (Rhoads et al., 2010; Wörle-Knirsch et al., 2007). When V<sub>2</sub>O<sub>5</sub> (rod-type, 50 ± 20 nm) and VO<sub>2</sub> (spherical type, 30 ± 10 nm) NPs were inhaled via a nose-only system for 2 weeks (0.1, 0.25, and 0.5 mg/m<sup>3</sup>, 6 h/day, 5 days/week), VO<sub>2</sub> NP-exposed rats showed higher levels of lactate dehydrogenase (LDH), gamma glutamyl transferase (gamma-GT), and alkaline phosphatase (ALP) compared to V<sub>2</sub>O<sub>5</sub> NP-exposed rats (Kulkarni et al., 2014). Evaluation on the levels of oxidative stress markers (malondialdehyde and reduced glutathione) also demonstrated a higher toxic potential of VO<sub>2</sub> NPs in this model. These changes became close to normal levels only in the V<sub>2</sub>O<sub>5</sub>-exposed rats after a 7-day recovery period. Additionally, histopathological damage and inflammatory responses were greater in the lung of VO<sub>2</sub> NP-exposed rats, and these changes persisted even after a 7-day recovery period. Meanwhile, increasing reports show that VO NPs have different dissolution rates in water based on their oxidation state (Bock et al., 2013; Brûyère et al., 1999; Larsson et al., 2015), and that dissolution rates can be an important factor determining the toxicity of NPs through disturbance of ion homeostasis in the body (Holmes et al., 2016; Ivask et al., 2014; Wang et al., 2016; Zhang et al., 2016). In this study, we aimed to identify the physicochemical properties that determine the toxicity of VO NPs by comparing the biological effects and tissue distribution of different types of VO NPs administered to mice, thus prepared five types of VO NPs, commercial (C)-VO<sub>2</sub> and -V<sub>2</sub>O<sub>5</sub> NPs and synthetic (S)-VO<sub>2</sub>, -V<sub>2</sub>O<sub>3</sub>, and -V<sub>2</sub>O<sub>5</sub> NPs. According to previous studies, LD<sub>50</sub> values for V<sub>2</sub>O<sub>5</sub> and other pentavalent vanadium compounds ranged from 10 to 160 mg/kg bw, and those for tetravalent vanadium compounds were in the range 448–467 mg/kg bw when orally dosed in mice (WHO, 2001). In addition, acute clinical symptoms were observed in animals exposed to 1 mg/m<sup>3</sup> concentration of V<sub>2</sub>O<sub>5</sub> (ATSDR, 2012). Moreover, the upper limit dose volume of 10 mL/kg is recommended for oral dosing in terms of animal welfare. Considering that dissolution rate can be influenced by pH condition, and that health effects by oral dosing can be more affected by pH compared to other exposure routes such as inhalation, skin and blood stream, we administered five types of VO NPs (1 mg/mL) with different properties by gavage (70 and 210 µg/mouse, approximately, 2 and 6 mg/kg, 6 days/week, 1 time/day) for 28 days, and then compared their tissue distributions and biological effects.

## 2. Materials and methods

### 2.1. Preparation of VO NPs

VO<sub>2</sub> NPs were synthesized via a one-step sol gel-assisted hydrothermal process (Shidong et al., 2011). V<sub>2</sub>O<sub>5</sub> (0.9 g, 99%, Sigma-Aldrich, St. Louis, MO, USA) powder was dissolved in a solution of 25 mL of deionized water (DW) and 5 mL of hydrogen peroxide (H<sub>2</sub>O<sub>2</sub>, 30 wt%, OCI Company, Seoul, Korea) with continuous stirring. After standing for 24 h, the V<sub>2</sub>O<sub>5</sub> solution turned into an amorphous gelatinous form. Then, a hydrazine monohydrate solution (N<sub>2</sub>H<sub>4</sub> · H<sub>2</sub>O; 98%, Sigma-Aldrich) was added to this gel under vigorous mixing. Within a few minutes, the gel turned to a black-colored stiffer gel. This resulting gel was transferred to a Teflon-lined stainless-steel autoclave and hydrothermally reacted at 220 °C for 24 h. After the hydrothermal reaction was completed, the obtained product was collected by centrifugation, thoroughly washed with DW and ethanol, and dried in a vacuum oven at 70 °C. To prepare the same size of V<sub>2</sub>O<sub>3</sub> and V<sub>2</sub>O<sub>5</sub> NPs, respectively, as-synthesized VO<sub>2</sub> NPs were heat-treated at 400 °C for 4 h in reduced atmosphere flowing H<sub>2</sub>(5%)/Ar mixed gas and 300 °C for 2 h in air atmosphere. We also purchased the commercial (C)-VO<sub>2</sub> (99%) and -V<sub>2</sub>O<sub>5</sub> (99.999%) powders purchased from Kojundo Co. and Alfa Aesar, respectively.

### 2.2. Characterization of vanadium oxides

All of S- and C-VO NPs were loaded in drinking water at a concentration of 1 mg/mL and sonicated using a bath-type sonicator (150 W, 40 kHz) for 5 min to disperse the VO NPs in a stable fashion. The temperature of the sonicator was kept below 30 °C to prevent agglomeration of particles. The phases and shapes of the S- and C-VO NPs were investigated using X-ray powder diffraction (XRD; D8-Advance, Bruker, Germany), transmission electron microscopy (TEM), and field emission scanning electron microscopy (FESEM; S-4800, Hitachi, Japan). The surface areas were estimated using a Brunauer–Emmett–Teller surface area analyzer (BET, ASAP2020, Furnace & Ceramics, Micrometrics Co., USA). In addition, the surface charge and hydrodynamic diameter (HDD) of the dispersed VO NPs were characterized using a Zeta Potential and Particle Size Analyzer (ELS-Z-1000, Otsuka Electronics Co. Ltd, Japan). Herein, we hypothesize that the particle size and interface effect related to solubility can be described by the Noyes–Whitney equation.

$$\frac{dC}{dt} = \frac{DA}{Vh} (C_s - C_x) \quad (1)$$

where  $dC/dt$  is dissolution rate,  $D$  is diffusion coefficient,  $A$  is surface area of the interface between the dissolving substance and the solvent,  $V$  is the volume of the dissolution medium,  $C_s$  is saturation solubility, and  $C_x$  is the mass concentration of the substance in the bulk of the solvent, and  $h$  = hydrodynamic boundary layer thickness.

### 2.3. Housing and VO NPs treatment

6-weeks old male ICR mice (specific pathogen free, 26–28 g, OrientBio, Seongnam, Korea) were housed at our specific pathogen free facility (23 ± 3 °C, relative humidity of 50 ± 10%, 12-h light/dark cycle [150–300 lx], and ventilation of 10–20 times/h) for 1 week before the initiation of experiment, a point water and food were supplied *ad libitum*. Five types of VO NPs were dosed by gavage (70 and 210 µg/mouse, approximately, 2 and 6 mg/kg and 6.5 mL/kg, 6 days/week, 1 time/day, 6 mice/group) for 28 days, and the control group was treated with sterilized drinking water. Body weight was checked one time per week. The experiments (IACUC

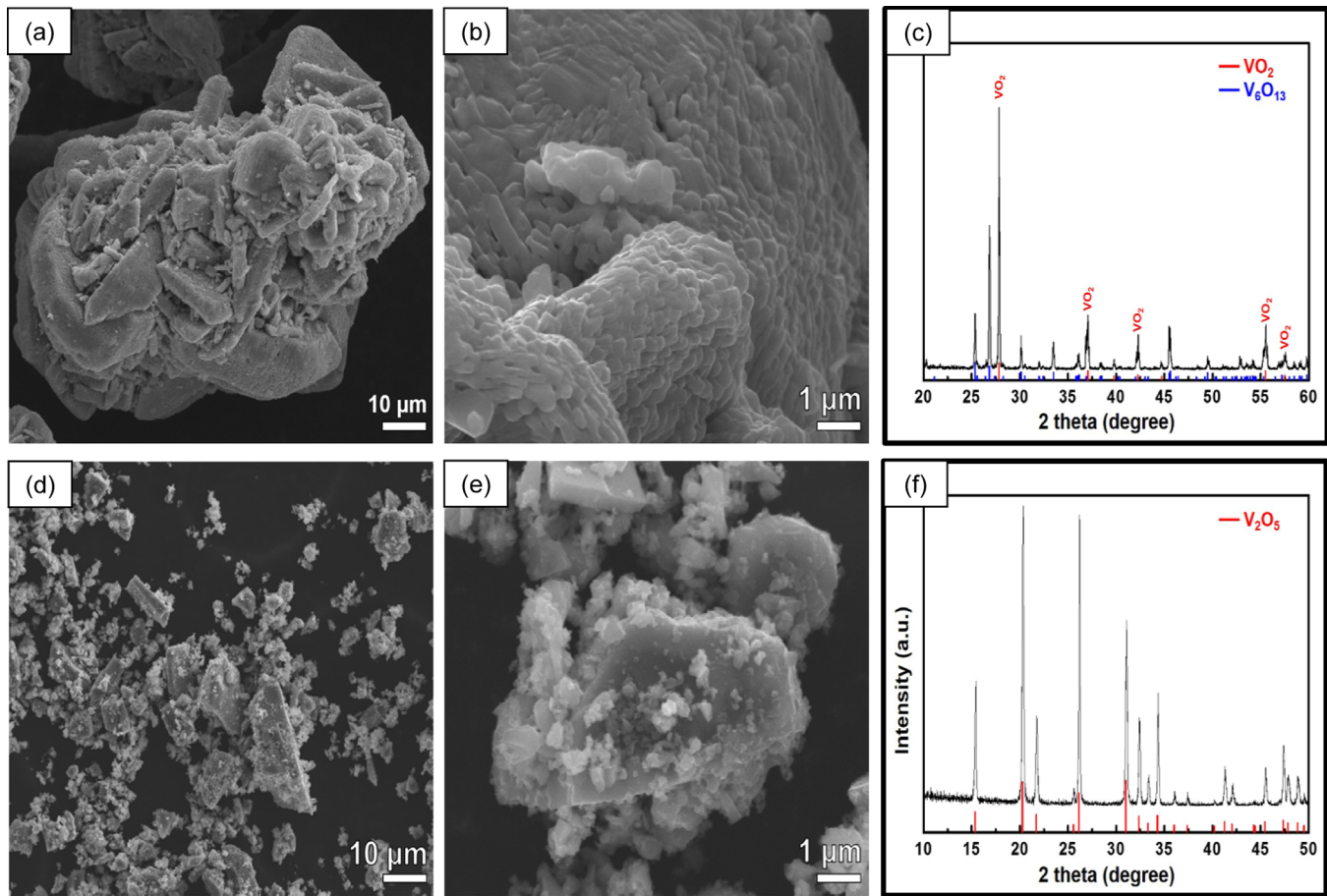


**Fig. 1.** (a,b) Typical FESEM images and (c) XRD pattern of C-VO<sub>2</sub>. (d,e) Typical FESEM images and (f) XRD pattern of C-V<sub>2</sub>O<sub>5</sub>.

No. 2014-0036) were assessed by the Institutional Animal Care and Committee (IACUC) of Ajou University (Suwon, Korea) and performed in accordance with the ILAR publication, "Guide for the Care and Use of Laboratory Animals."

#### 2.4. Blood analysis

All blood samples (6 samples/group, approximately 1.2 mL/mouse) were taken from the caudal vena cava, and a part of the whole blood was centrifuged at 3000 rpm for 10 min to obtain serum for biochemical analysis. Hematological and biochemical analysis were performed in Neodin Veterinary Science Institute (Seoul, Korea) using a blood autoanalyzer (HemaVet850, CDC Technologies, Inc., Dayton, Ohio, USA) and chemistry analyzer (BS-400, Mindray, Shenzhen, China), respectively.

#### 2.5. Trace elements and ion concentration measurement

The tissues (brain, thymus, lung, heart, liver, spleen, kidney, and testis) were collected after parturition. Tissues and blood (100 μL) were digested in a mixture of HNO<sub>3</sub> (70%, 7 mL) and H<sub>2</sub>O<sub>2</sub> (35%, 1 mL) solution using a microwave digestion system (Milestone, Sorisole, Italy) under high temperature (120 °C, 8 min; 50 °C, 2 min; 180 °C, 10 min) and high pressure. Finally, element (vanadium (V), copper (Cu), zinc (Zn), manganese (Mn), and iron (Fe)) concentrations in samples were measured according to the standard operating procedure using inductively coupled plasma mass spectrometry (ICP-MS) at the Korean Basic Science Institute (Table S1), and ion (electrolytes) concentrations in samples were evaluated using Inductively Coupled Plasma-Optical Emission

Spectrometer (ICP-OES, OPTIMA 5300DV, Perkin Elmer, USA) at Center for Materials Characterization and Machining, Ajou University (Table S2).

#### 2.6. Fate of VO NPs in the body

A part of blood and spleen of the mice were fixed in 2% glutaraldehyde in 0.1 M sodium cacodylate buffer (pH 7.2) for 2 h (Park et al., 2015). The tissues were then stained for 30 min in 0.5% aqueous uranyl acetate, dehydrated in graded ethanol solutions, and embedded in Spurr's resin. Thin sections were cut using an ultramicrotome (MT-X, RMC, Tucson, AZ, USA), stained with 2% uranyl acetate and Reynolds's lead citrate, and examined with a LIBRA 120 transmission electron microscope (Zeiss, Oberkochen, Germany) at an accelerating voltage of 80 kV.

#### 2.7. Immunophenotyping analysis

Splenocytes (6 mice/group) were isolated from spleen, which were collected at necropsy after repeated oral dosing for 28 days (Park et al., 2015). Briefly, spleens were ground in RPMI media containing fetal bovine serum (2%) and washed once with PBS. After removing red blood cells with FACS lysis buffer, splenocytes were filtered using a 70 μm-pore size nylon mesh, and then were resuspended in FACS buffer. Splenocytes were blocked with cluster of differentiation (CD)16/CD32 antibody (eBiosciences, San Diego, CA, USA) to reduce nonspecific binding, then incubated with the fluorescence dye labeled antibodies: phycoerythrin (PE)-conjugated anti-CD11b, fluorescein isothiocyanate (FITC)-conjugated anti-CD11c, FITC-conjugated anti-CD80 (B7-1), FITC-conjugated

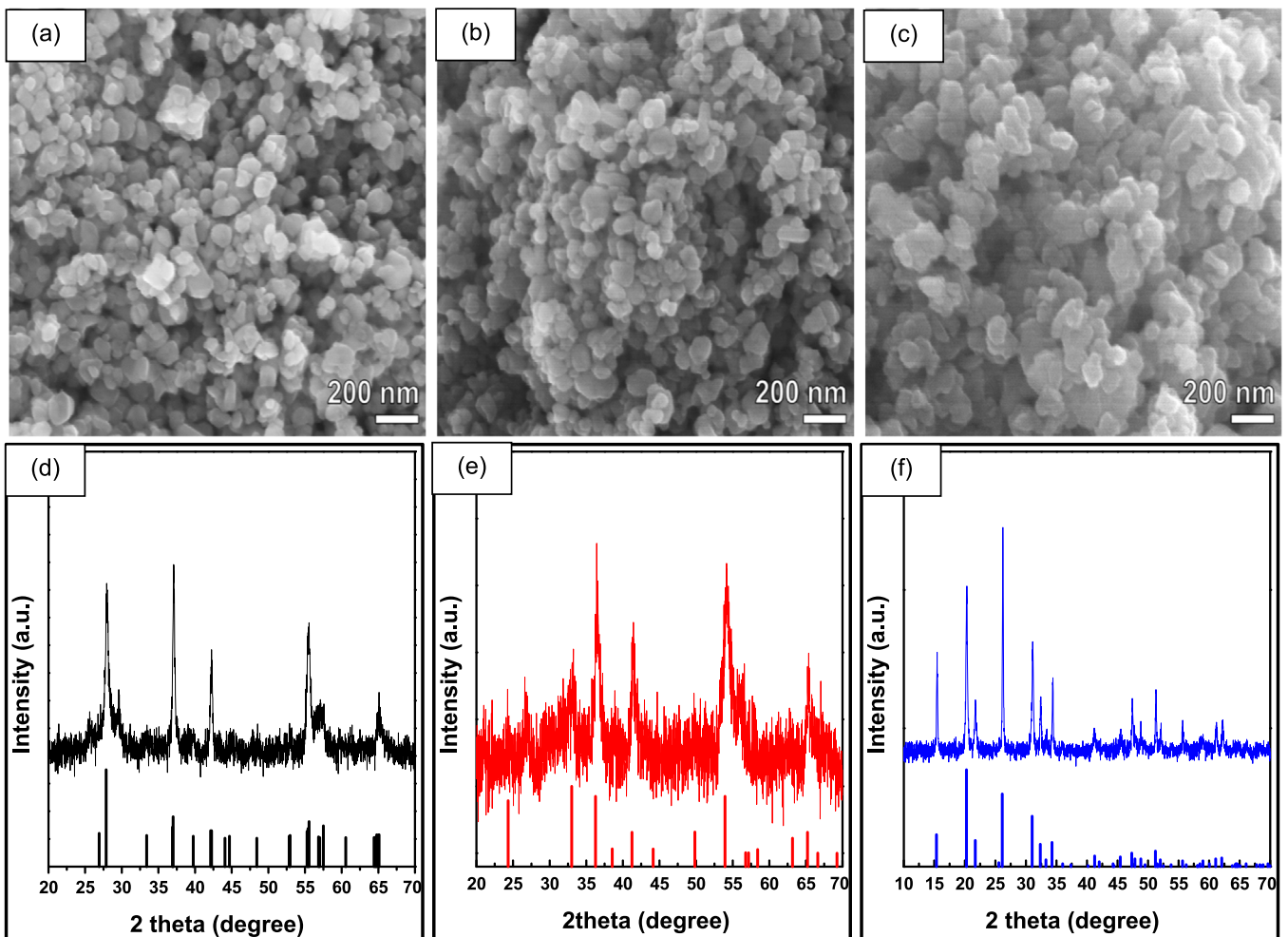


Fig. 2. Typical FESEM images of (a) S-VO<sub>2</sub>, (b) S-V<sub>2</sub>O<sub>3</sub>, and (c) S-V<sub>2</sub>O<sub>5</sub>. XRD patterns of (d) S-VO<sub>2</sub>, (e) S-V<sub>2</sub>O<sub>3</sub>, and (f) S-V<sub>2</sub>O<sub>5</sub>.

Table 1

A summary of the physicochemical characterization of VO NPs. S- and C-VO NPs were dispersed in autoclaved drinking water and each value is mean  $\pm$  SD of three independent measurements.

	HDD (nm)	Surface area ( $\text{m}^2 \text{g}^{-1}$ )	Pore volume ( $\text{cm}^3 \text{g}^{-1}$ )	Surface charge (mV)
C-VO <sub>2</sub>	Non-uniform (The most portion: $599.8 \pm 118.2$ )	0.34	0.0022	-6.8
C-V <sub>2</sub> O <sub>5</sub>	Non-uniform (The most portion: $435.2 \pm 29.8$ )	5.44	0.0469	-92.72
S-VO <sub>2</sub>	$138.5 \pm 0.4$	19.51	0.2147	-66.76
S-V <sub>2</sub> O <sub>3</sub>	$125.0 \pm 0.1$	19.66	0.2316	-31.9
S-V <sub>2</sub> O <sub>5</sub>	$170.5 \pm 0.9$	19.71	0.2483	-59.98

anti-CD3 (T cells), PE-conjugated anti-CD19 (B cells), APC-conjugated anti-DX5 (natural killer cells), FITC-conjugated anti-CD8 (cytotoxic T cells), PE-conjugated anti-CD4 (helper T cells) (eBioscience); and, APC-conjugated anti-CD86 (B7-2, BioLegend, Inc. San Diego, CA, USA) for 30 min at 4 °C according to the manufacturer's instructions. Then, cells were washed twice with FACS buffer and analyzed on a FACSCalibur (BD Biosciences, Franklin Lakes, NJ, USA) flow cytometer with CellQuest software.

## 2.8. Statistical analysis

All the results were mean  $\pm$  standard deviation (SD). To analyze statistical significance between the treated-group and the control group, Student's *t*-test and one way ANOVA test followed by

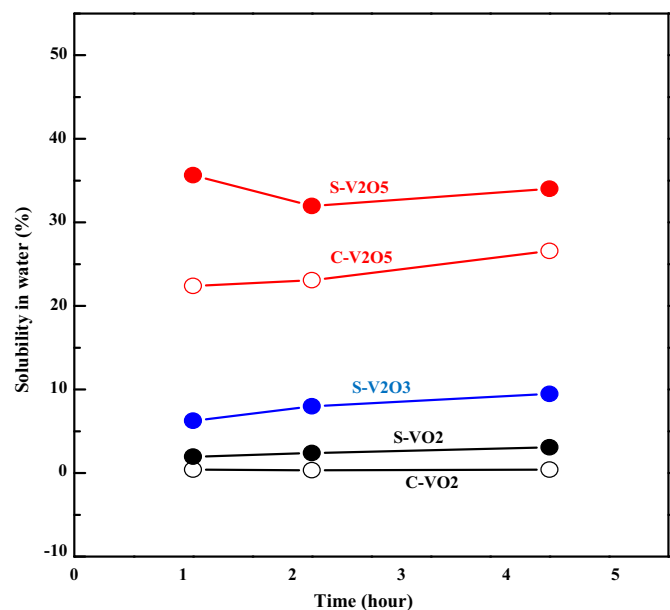
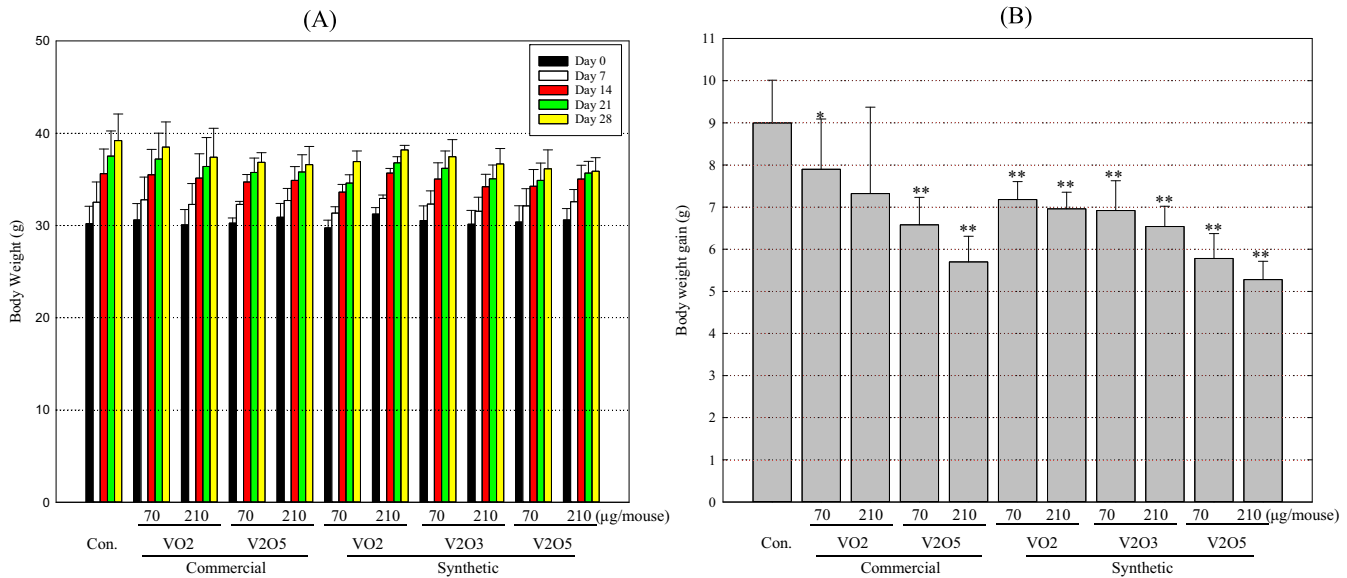
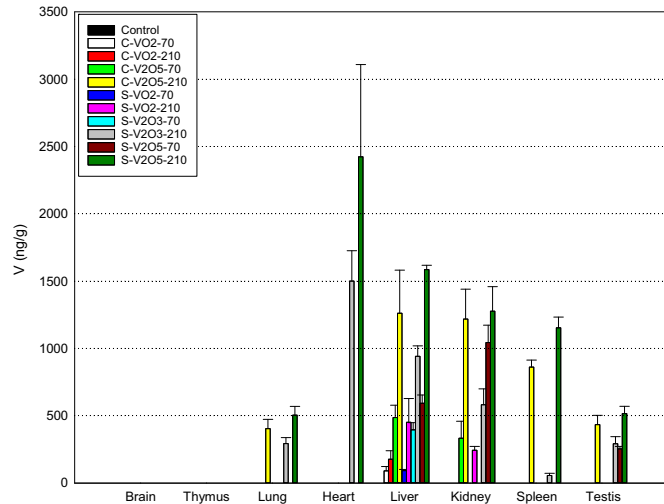


Fig. 3. Dissolution rate of five types of VO NPs in water.

Tukey's post hoc pairwise comparison (Graphpad Software, San Diego, CA, USA). *P* values of  $< 0.05$  were considered to be statistically significant.



**Fig. 4.** Comparison of body weight changes following repeated dosing of VO NPs. Body weight was measured one time per week from dosing (n=6). (A) Body weight (B) Body weight gain. \*\*p < 0.01.



**Fig. 5.** Vanadium level in tissues. Each tissue and blood were digested in a mixture of HNO<sub>3</sub> and H<sub>2</sub>O<sub>2</sub> solution (8 mL), and two lysates were pooled to make one sample for analysis (n=3). Results represent mean  $\pm$  SD. Vanadium was not detected all samples in the control group. All detected level showed statistical significance (\*\*p < 0.01).

### 3. Results

#### 3.1. Properties of VO NPs

C-VO<sub>2</sub> NPs exhibited strong aggregation and very large particle size of around 100 µm with irregular particle shapes (Fig. 1(a) and (b)) and could be indexed on mixed phases both the tetragonal VO<sub>2</sub> with a *P4<sub>2</sub>/mm* space group (PDF #74-1642) and the monoclinic V<sub>6</sub>O<sub>13</sub> with *C2/m* space group (PDF #89-0100) (Fig. 1(c)). C-VO<sub>2</sub> NPs are known to be a metastable oxide with a number of polymorphs (Bahlawane and Lenoble, 2014; Tsang and Manthiram, 1997). Pure VO<sub>2</sub> phase is very sensitive depending on the oxygen partial pressures and temperatures, which has the tendency of being over-oxidized V<sub>n</sub>O<sub>2n+1</sub> at the surface, as V<sub>6</sub>O<sub>13</sub> in air. These over-oxidized surface connect the three most common phases, V<sub>2</sub>O<sub>3</sub>, VO<sub>2</sub> and V<sub>2</sub>O<sub>5</sub> (Kang, 2012; Rampelberg, 2015). C-V<sub>2</sub>O<sub>5</sub> NPs also showed irregular particle shapes and sizes ranging from several hundreds of nanometers to several tens of micrometers

(Fig. 1(d) and (e)). They could be indexed on the basis of the orthorhombic V<sub>2</sub>O<sub>5</sub> with a *Pmmn* space group (PDF #41-1426) without any impurity phases (Fig. 1(f)). All synthesized VO (S-VO<sub>2</sub>, S-V<sub>2</sub>O<sub>3</sub>, and S-V<sub>2</sub>O<sub>5</sub>) NPs were homogeneous in size and shape (Fig. 2(a)–(c)). The HDDs of dispersed S-VO<sub>2</sub>, S-V<sub>2</sub>O<sub>3</sub>, and S-V<sub>2</sub>O<sub>5</sub> NPs were 138.50  $\pm$  0.40, 125.00  $\pm$  0.10, and 170.45  $\pm$  0.85 nm, respectively (Table 1). The XRD patterns of S-VO<sub>2</sub>, S-V<sub>2</sub>O<sub>3</sub>, and S-V<sub>2</sub>O<sub>5</sub> NPs highlighted their crystalline nature (Fig. 2(d)–(f)). S-VO<sub>2</sub> NPs showed the tetragonal VO<sub>2</sub> with a *P4<sub>2</sub>/mm* space group (PDF #74-1642, Fig. 2(d)), and S-V<sub>2</sub>O<sub>3</sub> NPs showed the hexagonal V<sub>2</sub>O<sub>3</sub> with an *R3c* space group (PDF #85-1411, Fig. 2(e)). Weak impurity peaks were observed for both S-VO<sub>2</sub> and S-V<sub>2</sub>O<sub>3</sub> NPs. S-V<sub>2</sub>O<sub>5</sub> NPs could be indexed on the basis of the orthorhombic V<sub>2</sub>O<sub>5</sub> with a *Pmmn* space group (PDF #41-1426), and exhibited higher purity and crystallinity than that exhibited by S-VO<sub>2</sub> and S-V<sub>2</sub>O<sub>3</sub> NPs (Fig. 2(f)). The dissolution rates of C- and S-V<sub>2</sub>O<sub>5</sub> NPs were higher ( $\geq 22.4\%$ ) compared to other VO NPs, with those of the C- and S-VO<sub>2</sub> NPs being very low ( $\leq 3\%$ ) (Fig. 3). The BET specific surface areas (SSA) of C-VO<sub>2</sub> and C-V<sub>2</sub>O<sub>5</sub> NPs were estimated to be 0.34 and 5.44 m<sup>2</sup>/g, respectively (Table 1). The three synthesized samples had similar BET SSA values ranging from 19.51 to 19.71 m<sup>2</sup>/g and pore volumes ranging from 0.2147 to 0.2483 cm<sup>3</sup>/g. Finally, all prepared samples in IPA exhibited a negative charge.

#### 3.2. Comparison of body weight change

It is known that one of the adverse health effects following administration of vanadium is a decrease of body weight. Thus, we measured body weight weekly and found that body weight significantly decreased following dosing of all types of VO NPs, except C-VO<sub>2</sub> NPs (Fig. 4(A)). The decreased level was the order of V<sub>2</sub>O<sub>5</sub> (S > C) > V<sub>2</sub>O<sub>3</sub> > VO<sub>2</sub> (S > C) NPs (Fig. 4(B)).

#### 3.3. Comparison of vanadium level in tissues

In general, the five types of VO NPs accumulated to the greatest extent in the liver and kidney with accumulation in the order of V<sub>2</sub>O<sub>5</sub> (S > C) > V<sub>2</sub>O<sub>3</sub> > VO<sub>2</sub> (S > C) (Fig. 5). S-V<sub>2</sub>O<sub>5</sub> NPs also accumulated in the heart, spleen, lung, and testis, and remained in the blood until 24 h after final dosing (Table S3). We additionally observed that S- and C-V<sub>2</sub>O<sub>5</sub> NPs can easily penetrate red blood cells

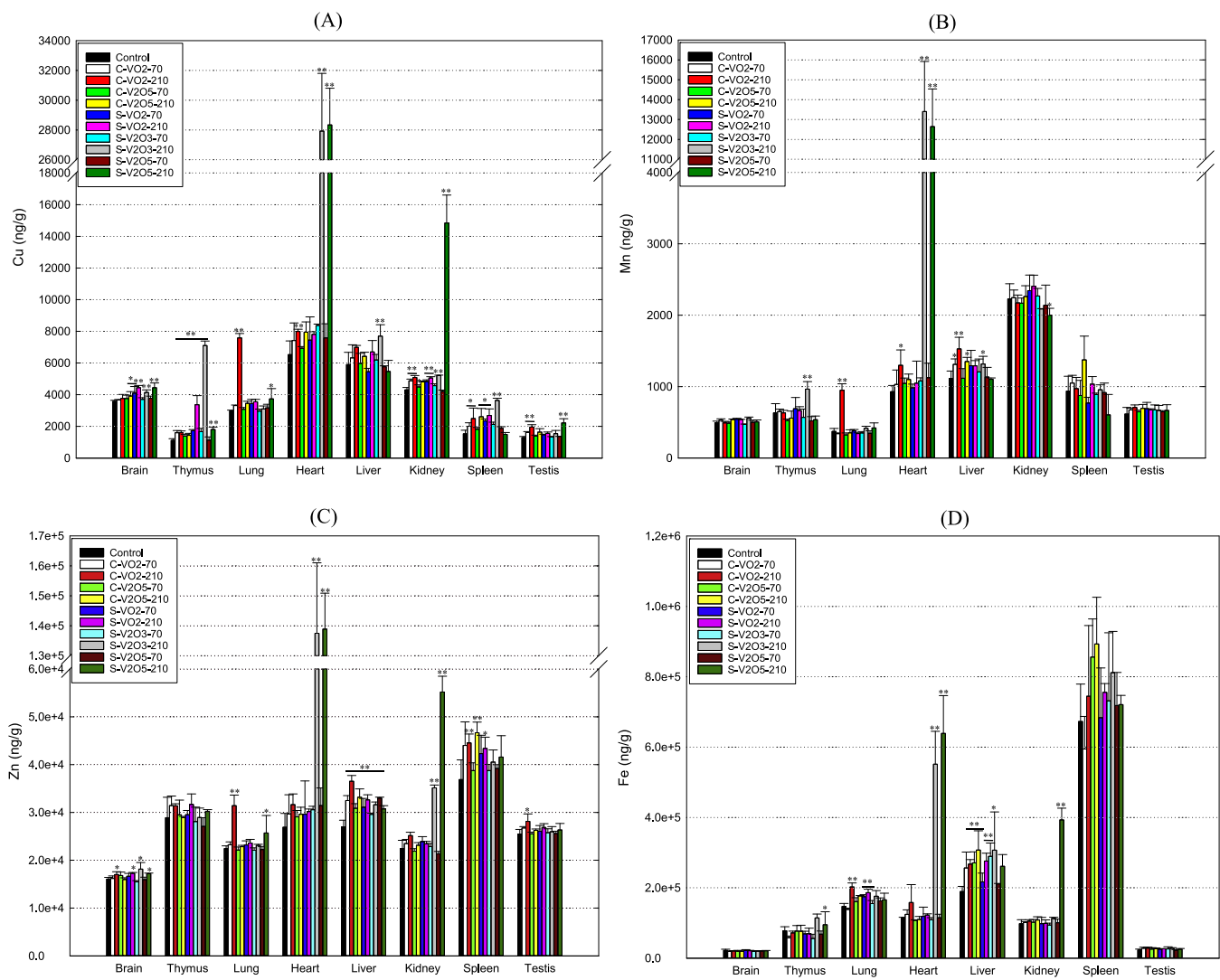


**Fig. 6.** Tissue level of redox-related trace elements. Results represent mean  $\pm$  SD (n=3). \*p < 0.05; \*\*p < 0.01. (A) Cu, (B) Mn, (C) Zn, (D) Fe.

(RBC, Fig. S1) and travel to the spleen (Fig. S2) 12 h after dosing. On the other hand, vanadium was not detected in brain and thymus samples from any of the VO NP-treated groups.

#### 3.4. Alteration of redox reaction-related trace element levels in tissues

Considering that metal oxide NPs can generate oxidative stress through the formation of free radicals (Zhang et al., 2012), we measured tissue levels of redox reaction-related elements including Cu, Mn, Zn and Fe (Fig. 6). Interestingly, when comparing the higher dose of VO NP groups with the control group, levels of trace elements were clearly altered to the greatest extent in the heart of mice exposed to S-V<sub>2</sub>O<sub>3</sub> and S-V<sub>2</sub>O<sub>5</sub> and in the kidneys of mice exposed to S-V<sub>2</sub>O<sub>5</sub>.

#### 3.5. Perturbation of electrolytes in tissues

Metal ions dissolved from NPs can influence the ionic (electrolyte) environment in the body. At the higher dose (210  $\mu$ g/mouse), the levels of sodium ions ( $Na^+$ ) were remarkably enhanced in the heart of mice exposed to S-V<sub>2</sub>O<sub>3</sub> and S-V<sub>2</sub>O<sub>5</sub> NPs compared to the control (Fig. 7(A)), levels of potassium ions ( $K^+$ ) were also clearly elevated in the heart of mice exposed to S-V<sub>2</sub>O<sub>3</sub> and S-V<sub>2</sub>O<sub>5</sub> NPs and in the kidneys of mice exposed to S-V<sub>2</sub>O<sub>5</sub> NPs

(Fig. 7(B)). Meanwhile, very interestingly, the different five types of VO NPs altered levels of calcium ions ( $Ca^{2+}$ ) in all tissues evaluated (Fig. 7(C)).

#### 3.6. Comparison of systemic health effects following accumulation of VO NPs

At the higher dose (210  $\mu$ g/mouse), S-V<sub>2</sub>O<sub>3</sub> NPs significantly decreased levels of total protein, albumin, and glucose in the blood as compared to the control, and S-V<sub>2</sub>O<sub>5</sub> NPs clearly reduced levels of total protein, albumin, and amylase (Table 2). Meanwhile,  $K^+$  levels were notably inhibited in all treatment groups, except the S-V<sub>2</sub>O<sub>5</sub> NP group. Moreover, the levels of white blood cells (WBC) significantly decreased in all treatment groups exposed to the higher dose compared to the control, whereas the proportion of monocytes showed a remarkable reduction in the blood of mice exposed to the higher dose of C- and S-V<sub>2</sub>O<sub>5</sub>, and S-V<sub>2</sub>O<sub>3</sub> NPs (Table 3). Considering that exposure to vanadium can influence the host immune system (Ha et al., 2012; Ustarroz-Cano et al., 2012), and that acquired immune response may be dominant according to repeated exposure, we compared effects on function of antigen-presenting cells (APCs), main players in acquired immune response. At 210  $\mu$ g/mouse, co-expression of CD80 and CD86 was inhibited in all treated-groups compared to the control, and the inhibited level was in the order of S-V<sub>2</sub>O<sub>5</sub> > C-V<sub>2</sub>O<sub>5</sub> > S-V<sub>2</sub>O<sub>3</sub> > S-VO<sub>2</sub> > C-VO<sub>2</sub> NPs (Fig. 8(A)).

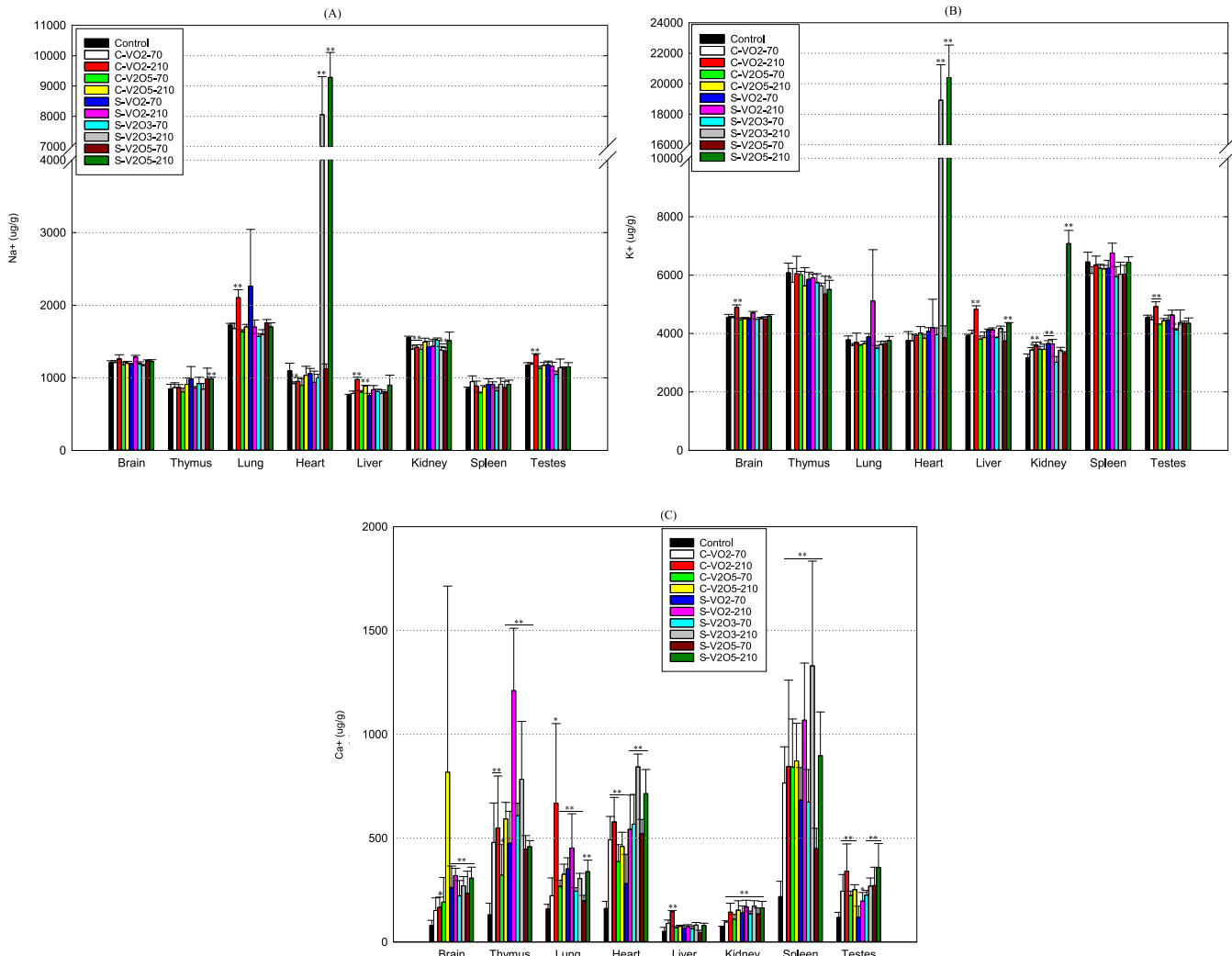


Fig. 7. Changes of electrolytes following repeated dosing of VO NPs. Results represent mean  $\pm$  SD ( $n=3$ ). \* $p < 0.05$ ; \*\* $p < 0.01$ . (A)  $\text{Na}^+$ , (B)  $\text{K}^+$ , (C)  $\text{Ca}^{2+}$ .

Meanwhile, maturation of dendritic cells ( $\text{CD11b}^-/\text{CD11c}^+$ ) was significantly decreased only in mice administered with the higher dose of S- $\text{V}_2\text{O}_5$  NPs (Fig. 8(A)). Moreover, as compared to the control, the relative portion of splenic T cells was clearly elevated following dosing of four types of VO NPs (210  $\mu\text{g}/\text{mouse}$ , Fig. 8(B)), except C- $\text{VO}_2$  NPs, by an increase of helper T cells (CD4 T, Fig. 8(C)).

#### 4. Discussion

With the increasing use of nanotechnology across a wide range of applications, considerable effort has been devoted to understanding the main issues in nano-toxicology that may account for the potential adverse effects of NPs to humans and the environment (Sabella et al., 2014). Accumulating evidence has shown that the biopersistence and associated biological effects of metal-containing NPs are controlled by various factors including size, shape, crystal structure, oxidation state, dissolution rate, and raw material components (Aust et al., 2011; Borm et al., 2006; Cho et al., 2013), and that dissolution which means release of ions from NPs has been used to evaluate biodurability of NPs (Utembe et al., 2015; Wiecinski et al., 2009). Namely, if NPs are rapidly ionized, their short-term toxic effects can be determined by the nature of the dissolved ions. However, if NPs are slowly ionized, the potential effects may depend on the nature of the NPs themselves.  $\text{V}_2\text{O}_5$  was classified as a Group 2B (possible) human carcinogen by

the U.S. National Toxicology Program (IARC, 2006). However, we cannot extend this conclusion to all vanadium compounds based on  $\text{V}_2\text{O}_5$  toxicity data alone because the toxicity of some vanadium species may differ based on their different properties. For example, they may differ in the degree to which they can generate reactive oxygen species and induce subsequent toxicity effects (Valko et al., 2005). Additionally, vanadium in one particular form could be bioconverted *in vivo* to an other undefined toxic species (Duffus, 2007).

Vanadium can form a range of various binary oxides with the general formula  $\text{VO}_{2+x}$  ( $0 \leq x \leq 0.33$ ), including  $\text{VO}_2$ ,  $\text{V}_2\text{O}_3$ ,  $\text{V}_6\text{O}_{13}$ , and  $\text{V}_2\text{O}_5$  (Chen et al., 2004; Tsang and Manthiram, 1997). These crystal structures consist of distorted octahedral  $\text{VO}_6$ , which share both corners and edges (Tsang and Manthiram, 1997). Additionally, because  $\text{V}_2\text{O}_5$  is soluble in water, it can dissolve when in contact with moisture in living organisms or ecosystems and thereby produce a variety of dissolved vanadium species of different oxidation states ( $\text{V}^{3+}$ ,  $\text{V}^{4+}$ , and  $\text{V}^{5+}$ ) (ATSDR, 2012; WHO, 2001). We note that water solubility of  $\text{V}_2\text{O}_5$  is highest among VO NPs and water solubility is increased as exposure surface of VO NPs increase. The solubility of S-VO NPs of smaller particle size was greater compared to C-VO NPs of larger particle size. S-VO NPs had large BET SSA values ( $> 19 \text{ m}^2/\text{g}$ ) and large pore volumes ( $> 0.2 \text{ cm}^3/\text{g}$ ), compared with their values of C-VO NPs.

Growing evidences show that administered VO NPs could be distributed to other organs via various routes leading to systemic

**Table 2**

Biochemical changes in the blood of mice dosed with VO NPs. Blood (6 mice/group, n=6) was collected 24 h after final dosing. Results represent mean  $\pm$  SD. \*p < 0.05; \*\*p < 0.01. TP; Total protein, TBil; Total bilirubin, Cr; Creatinine, AST; Aspartate aminotransferase, ALT; Alanine aminotransferase, ALP; Alkaline phosphatase,  $\gamma$ -GTP; Gamma-glutamyl transferase, Na; Sodium, K; Potassium, Cl; Chloride.

Name	TP	Albumin	TBil	Glucose	BUN	Cr	AST	ALT	ALP	$\gamma$ -GTP	Amylase	Globulin	Na	K	Cl
Unit	g/dL	g/dL	mg/dL	mg/dL	mg/dL	mg/dL	U/L	U/L	U/L	U/L	U/L	g/dL	mmol/L	mmol/L	mmol/L
Control	5.9 $\pm$ 0.1	3.7 $\pm$ 0.1	0.2 $\pm$ 0.0	350.3 $\pm$ 54.7	21.3 $\pm$ 0.8	0.3 $\pm$ 0.0	57.3 $\pm$ 4.6	31.0 $\pm$ 4.3	78.7 $\pm$ 3.7	0.0 $\pm$ 0.0	3768.6 $\pm$ 396.5	2.2 $\pm$ 0.0	153.2 $\pm$ 1.2	8.6 $\pm$ 0.2	110.8 $\pm$ 1.6
C-VO <sub>2</sub> (70)	5.9 $\pm$ 0.2	3.4 $\pm$ 0.1	0.2 $\pm$ 0.0	277.3 $\pm$ 7.4	20.9 $\pm$ 1.3	0.3 $\pm$ 0.0	62.0 $\pm$ 2.2	36.7 $\pm$ 1.7	77.7 $\pm$ 21.1	0.0 $\pm$ 0.0	3667.2 $\pm$ 290.0	2.5 $\pm$ 0.1	157.7 $\pm$ 1.3	6.1 $\pm$ 0.3**	115.8 $\pm$ 0.5
C-VO <sub>2</sub> (210)	5.8 $\pm$ 0.1	3.4 $\pm$ 0.2	0.2 $\pm$ 0.0	257.3 $\pm$ 40.4	22.0 $\pm$ 0.5	0.3 $\pm$ 0.0	73.7 $\pm$ 7.6	39.7 $\pm$ 2.9	71.0 $\pm$ 16.7	0.0 $\pm$ 0.0	3747.0 $\pm$ 401.3	2.4 $\pm$ 0.1	157.8 $\pm$ 0.6	6.8 $\pm$ 0.8**	116.3 $\pm$ 1.2
C-V <sub>2</sub> O <sub>5</sub> (70)	5.8 $\pm$ 0.2	3.4 $\pm$ 0.2	0.2 $\pm$ 0.0	275.0 $\pm$ 16.4*	20.9 $\pm$ 0.4	0.2 $\pm$ 0.0	59.0 $\pm$ 8.5	35.3 $\pm$ 8.3	77.3 $\pm$ 19.3	0.0 $\pm$ 0.0	3170.3 $\pm$ 94.8	2.4 $\pm$ 0.0**	153.4 $\pm$ 0.2	6.6 $\pm$ 0.5**	112.6 $\pm$ 1.3
C-V <sub>2</sub> O <sub>5</sub> (210)	5.7 $\pm$ 0.1	3.4 $\pm$ 0.1	0.2 $\pm$ 0.0	262.3 $\pm$ 91.7	21.9 $\pm$ 0.5	0.2 $\pm$ 0.1	64.3 $\pm$ 12.4	33.7 $\pm$ 6.2	91.3 $\pm$ 11.9	0.0 $\pm$ 0.0	2959.5 $\pm$ 414.9	2.3 $\pm$ 0.0	156.9 $\pm$ 1.7	6.9 $\pm$ 0.7**	114.5 $\pm$ 2.7
S-VO <sub>2</sub> (70)	5.8 $\pm$ 0.1	3.3 $\pm$ 0.0	0.2 $\pm$ 0.0	309.8 $\pm$ 18.6	18.8 $\pm$ 0.8	0.2 $\pm$ 0.0	45.5 $\pm$ 4.2	33.8 $\pm$ 8.6	74.3 $\pm$ 7.4	0.0 $\pm$ 0.0	3252.3 $\pm$ 116.4	2.5 $\pm$ 0.1	154.1 $\pm$ 0.5	5.4 $\pm$ 0.2**	110.4 $\pm$ 0.5
S-VO <sub>2</sub> (210)	5.9 $\pm$ 0.3	3.5 $\pm$ 0.2	0.2 $\pm$ 0.0	281.5 $\pm$ 32.2	23.2 $\pm$ 1.4	0.3 $\pm$ 0.1	48.5 $\pm$ 11.9	29.5 $\pm$ 6.2	63.0 $\pm$ 4.9**	0.0 $\pm$ 0.0	3441.1 $\pm$ 397.7	2.4 $\pm$ 0.3	154.2 $\pm$ 0.9	6.0 $\pm$ 1.4**	111.7 $\pm$ 1.9
S-V <sub>2</sub> O <sub>3</sub> (70)	5.7 $\pm$ 0.2	3.3 $\pm$ 0.1	0.2 $\pm$ 0.0	253.3 $\pm$ 22.1**	26.8 $\pm$ 3.0	0.2 $\pm$ 0.0	55.3 $\pm$ 9.7	27.3 $\pm$ 1.9	63.3 $\pm$ 8.2**	0.0 $\pm$ 0.0	3068.3 $\pm$ 162.7	2.4 $\pm$ 0.2	154.6 $\pm$ 0.8	6.6 $\pm$ 0.9**	113.6 $\pm$ 0.1
S-V <sub>2</sub> O <sub>3</sub> (210)	5.4 $\pm$ 0.2**	3.2 $\pm$ 0.1**	0.3 $\pm$ 0.0	219.7 $\pm$ 53.3**	21.2 $\pm$ 2.4	0.1 $\pm$ 0.1	46.3 $\pm$ 7.6	22.3 $\pm$ 0.5**	85.0 $\pm$ 7.8	0.0 $\pm$ 0.0	2526.9 $\pm$ 273.5	2.2 $\pm$ 0.2	152.5 $\pm$ 1.5	6.1 $\pm$ 0.6**	112.6 $\pm$ 0.7
S-V <sub>2</sub> O <sub>5</sub> (70)	6.0 $\pm$ 0.2	3.8 $\pm$ 0.3	0.1 $\pm$ 0.0	392.0 $\pm$ 62.1	24.8 $\pm$ 1.7	0.3 $\pm$ 0.0	60.7 $\pm$ 5.2	25.7 $\pm$ 0.5	68.7 $\pm$ 7.4	0.0 $\pm$ 0.0	3153.6 $\pm$ 110.8	2.8 $\pm$ 0.3**	152.5 $\pm$ 1.1	10.0 $\pm$ 1.0*	110.6 $\pm$ 0.4
S-V <sub>2</sub> O <sub>5</sub> (210)	5.4 $\pm$ 0.0**	3.2 $\pm$ 0.1**	0.1 $\pm$ 0.0	379.3 $\pm$ 33.0	29.2 $\pm$ 2.2	0.3 $\pm$ 0.1	48.3 $\pm$ 7.4	26.0 $\pm$ 4.5	71.3 $\pm$ 9.2	0.0 $\pm$ 0.0	2647.8 $\pm$ 151.1**	2.2 $\pm$ 0.1	155.0 $\pm$ 0.7	7.8 $\pm$ 1.0	113.7 $\pm$ 1.2

**Table 3**

Hematological changes in the blood of mice dosed with VO NPs. WBC, white blood cells; LY, lymphocytes; MO, monocytes; NE, neutrophils; EO, eosinophils; BA, basophils; RBC, red blood cells; MCV, mean corpuscular volume; HCT, hematocrit; MCH, mean corpuscular hemoglobin; MCHC, mean corpuscular hemoglobin concentration; Hgb, hemoglobin; RDW, red blood cell distribution width; PLT, platelet; MPV, mean platelet volume.

Name	WBC	LY	MO	NE	EO	BA	RBC	MCV	HCT	MCH	MCHC	Hgb	RDW	PLT	MPV
Unit	K/uL	%	%	%	%	%	M/mm <sup>3</sup>	fL	%	pg	g/dL	g/dL	%	K/uL	fL
Control	3.2 $\pm$ 1.1	82.0 $\pm$ 3.5	4.1 $\pm$ 1.7	10.7 $\pm$ 5.6	2.4 $\pm$ 0.5	0.7 $\pm$ 0.6	8.2 $\pm$ 0.4	48.6 $\pm$ 1.7	40.1 $\pm$ 3.3	18.2 $\pm$ 0.4	37.4 $\pm$ 1.4	14.9 $\pm$ 0.8	18.3 $\pm$ 0.3	833.5 $\pm$ 195.7	9.1 $\pm$ 0.8
C-VO <sub>2</sub> (70)	1.3 $\pm$ 0.4	81.4 $\pm$ 1.1	1.2 $\pm$ 0.5**	14.7 $\pm$ 1.2	1.7 $\pm$ 0.4	0.7 $\pm$ 0.4	8.7 $\pm$ 0.5	46.5 $\pm$ 2.2	41.0 $\pm$ 1.9	17.7 $\pm$ 0.4	40.3 $\pm$ 5.9	14.1 $\pm$ 2.7	18.4 $\pm$ 0.4	1149.0 $\pm$ 103.7	9.6 $\pm$ 0.7
C-VO <sub>2</sub> (210)	1.0 $\pm$ 0.4**	78.6 $\pm$ 5.8	2.9 $\pm$ 1.7	18.1 $\pm$ 4.3	2.4 $\pm$ 0.3	1.1 $\pm$ 0.5	8.2 $\pm$ 0.3	50.3 $\pm$ 2.2	41.4 $\pm$ 1.8	16.4 $\pm$ 2.0	32.7 $\pm$ 4.0	13.5 $\pm$ 1.6	17.7 $\pm$ 0.5	1018.3 $\pm$ 128.1	8.7 $\pm$ 0.3
C-V <sub>2</sub> O <sub>5</sub> (70)	1.5 $\pm$ 0.8	80.8 $\pm$ 4.9	2.1 $\pm$ 1.1	17.1 $\pm$ 3.5	2.8 $\pm$ 1.5	0.7 $\pm$ 0.3	7.8 $\pm$ 0.7	48.7 $\pm$ 1.7	37.8 $\pm$ 4.2	17.8 $\pm$ 0.6	36.5 $\pm$ 0.5	13.8 $\pm$ 1.5	17.8 $\pm$ 0.5	821.0 $\pm$ 95.8	9.1 $\pm$ 0.7
C-V <sub>2</sub> O <sub>5</sub> (210)	0.8 $\pm$ 0.3**	79.0 $\pm$ 2.6	1.2 $\pm$ 0.2**	15.6 $\pm$ 1.3	2.8 $\pm$ 1.0	1.1 $\pm$ 0.2	7.8 $\pm$ 1.0	48.3 $\pm$ 1.5	37.7 $\pm$ 4.3	17.9 $\pm$ 1.4	37.1 $\pm$ 2.7	13.9 $\pm$ 1.0	17.8 $\pm$ 0.3	806.5 $\pm$ 35.0	9.4 $\pm$ 1.5
S-VO <sub>2</sub> (70)	2.3 $\pm$ 0.6	82.1 $\pm$ 4.9	3.1 $\pm$ 1.3	11.5 $\pm$ 5.2	2.1 $\pm$ 0.7	0.9 $\pm$ 0.2	8.0 $\pm$ 1.1	49.2 $\pm$ 2.4	42.9 $\pm$ 2.7	19.5 $\pm$ 3.0	39.7 $\pm$ 6.0	15.6 $\pm$ 3.4	17.8 $\pm$ 0.4	814.0 $\pm$ 176.8	8.7 $\pm$ 0.4
S-VO <sub>2</sub> (210)	1.4 $\pm$ 0.7**	81.6 $\pm$ 4.1	3.6 $\pm$ 1.8	11.5 $\pm$ 6.0	2.4 $\pm$ 1.1	0.7 $\pm$ 0.7	7.9 $\pm$ 1.2	49.2 $\pm$ 3.3	38.9 $\pm$ 6.8	17.9 $\pm$ 1.4	36.4 $\pm$ 2.2	14.0 $\pm$ 2.1	18.1 $\pm$ 0.8	1023.8 $\pm$ 199.0	8.2 $\pm$ 0.5
S-V <sub>2</sub> O <sub>3</sub> (70)	1.8 $\pm$ 1.0	79.7 $\pm$ 5.9	2.9 $\pm$ 1.1	16.3 $\pm$ 4.7	2.1 $\pm$ 0.8	1.0 $\pm$ 0.7	8.9 $\pm$ 0.6	50.4 $\pm$ 1.1	45.0 $\pm$ 3.2	17.3 $\pm$ 0.6	34.3 $\pm$ 1.5	15.4 $\pm$ 0.8	18.2 $\pm$ 0.5	1074.3 $\pm$ 260.9	7.9 $\pm$ 1.0
S-V <sub>2</sub> O <sub>3</sub> (210)	1.0 $\pm$ 0.9**	79.1 $\pm$ 2.6	1.8 $\pm$ 0.2**	16.5 $\pm$ 2.4	2.5 $\pm$ 0.9	0.7 $\pm$ 0.4	7.7 $\pm$ 1.4	48.6 $\pm$ 2.3	37.5 $\pm$ 7.5	17.7 $\pm$ 1.9	34.7 $\pm$ 2.6	13.4 $\pm$ 1.5	18.1 $\pm$ 0.5	932.6 $\pm$ 223.1	8.4 $\pm$ 1.0
S-V <sub>2</sub> O <sub>5</sub> (70)	1.6 $\pm$ 1.6	80.9 $\pm$ 6.0	2.1 $\pm$ 0.9	15.4 $\pm$ 7.2	1.5 $\pm$ 0.7	0.4 $\pm$ 0.4	8.4 $\pm$ 0.8	46.7 $\pm$ 2.6	39.3 $\pm$ 5.3	16.4 $\pm$ 0.6	35.2 $\pm$ 1.9	13.8 $\pm$ 1.4	18.8 $\pm$ 0.6	1004.8 $\pm$ 349.9	10.3 $\pm$ 1.3
S-V <sub>2</sub> O <sub>5</sub> (210)	0.9 $\pm$ 0.5**	83.4 $\pm$ 5.1	1.3 $\pm$ 0.9**	12.5 $\pm$ 5.1	1.7 $\pm$ 0.9	0.9 $\pm$ 0.2	7.6 $\pm$ 1.8	48.2 $\pm$ 3.3	36.9 $\pm$ 9.7	15.8 $\pm$ 2.2	32.9 $\pm$ 5.5	12.4 $\pm$ 4.1	18.1 $\pm$ 0.7	614.3 $\pm$ 274.6	11.5 $\pm$ 1.8

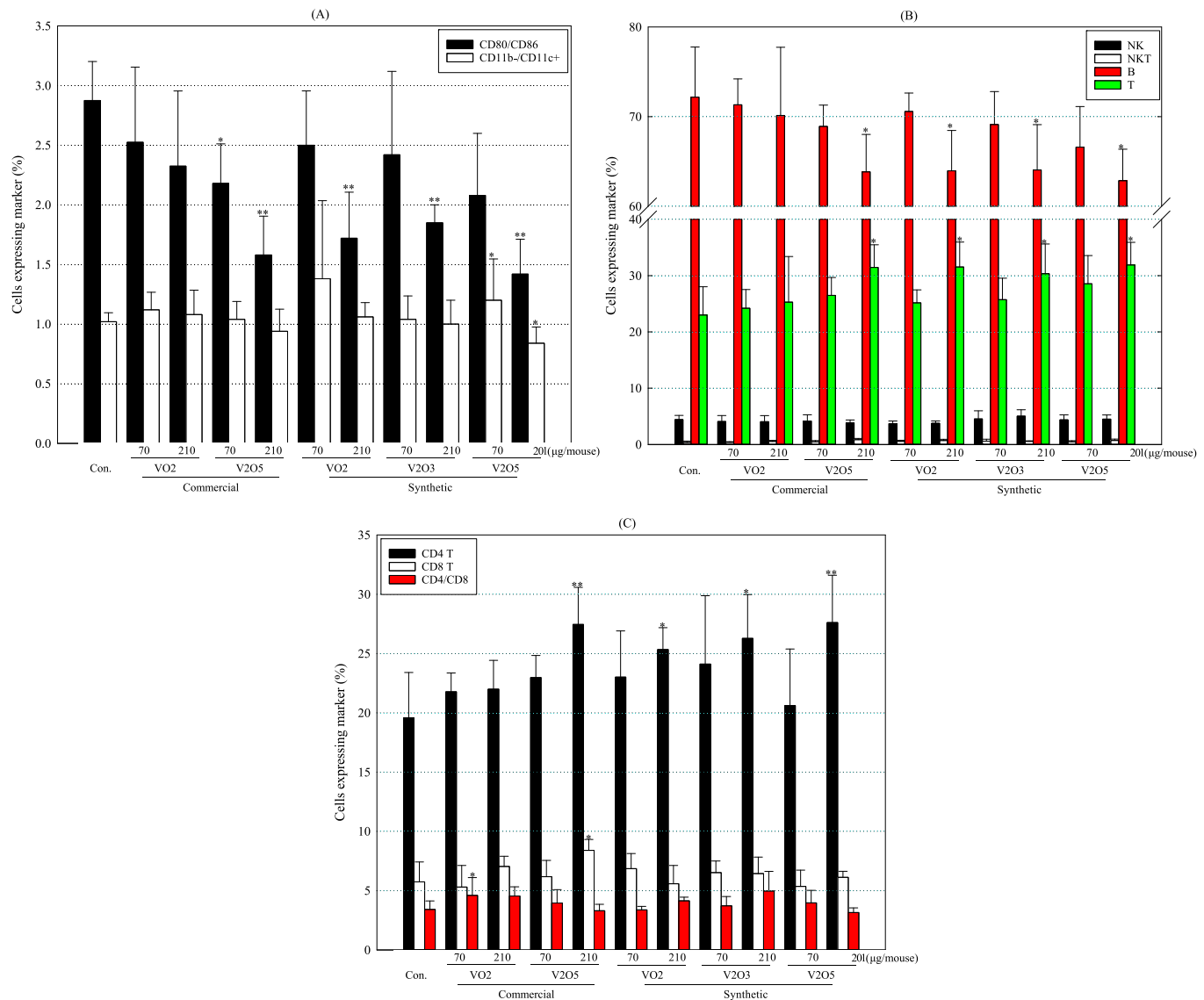


**Fig. 8.** Immunotoxic response following accumulation of VO NPs. 10,000 cells per sample (6 samples/group) were counted. \* $p < 0.05$ , \*\* $p < 0.01$ . (A) Antigen presentation-related markers. "CD11b<sup>-</sup>/CD11c<sup>+</sup>" indicates the maturation of dendritic cells, (B) cell distribution, (C) constituents of T cells.

effects. For instance, vanadium exposure to diabetic mice has been shown to affect the level of redox reaction-related elements and ions (electrolytes) in different tissues (Krośniak et al., 2013). Inhaled vanadium also inhibited maturation of thymic dendritic cells (Ustarroz-Cano et al., 2012). Additionally, in a study evaluating vanadium as an alternative therapy to parenteral insulin in diabetic patients, the observed adverse effects depended on circulating levels of vanadium (Domingo, 1996). In our study, C- and S-V<sub>2</sub>O<sub>5</sub> and S-V<sub>2</sub>O<sub>3</sub> NPs were detected in the blood until 24 h after final dosing, although they were trace amounts (Table S3). We could also observe that S- and C-V<sub>2</sub>O<sub>5</sub> NPs penetrate into RBC and travel to the spleen on 12 h after dosing. Moreover, S-V<sub>2</sub>O<sub>5</sub> and S-V<sub>2</sub>O<sub>3</sub> NPs more accumulated in tissues compared to other VO NPs, and the accumulated level was in order of the heart > liver > kidney > spleen. Homeostasis of ions (electrolytes), such as Na<sup>+</sup>, K<sup>+</sup>, and Ca<sup>2+</sup>, is essential for living organisms, especially with respect to cell physiology and function, and an ion levels in tissue (or cells) can influence the level of other ions (Barros et al., 2002; Restrepo-Angulo et al., 2010; Shattock et al., 2015; Yang et al., 2015). For example, Na<sup>+</sup> overload is closely correlated with the generation of ischemic heart (Takeo and

Tanonaka, 2004). Intracellular Ca<sup>2+</sup> overload can lead to oxidative stress and apoptosis in a range of cell-types, thereby promoting the development of several diseases (Övey and Naziroğlu, 2015; Santulli et al., 2015). In addition, some researchers have suggested that VO NPs can induce toxicity by triggering oxidative stress via generation of reactive oxygen species (Fickl et al., 2006; Kulkarni et al., 2014; Wörle-Knirsch et al., 2007). For example, in a study comparing toxicity of V<sub>2</sub>O<sub>3</sub> and V<sub>2</sub>O<sub>5</sub> particles of nano- and micro-sized using various cells, VO NPs showed stronger toxicity compared to the corresponding micro-sized particles by generating the higher oxidative stress, and the observed effects could be explained by both oxidation state and size (Wörle-Knirsch et al., 2007). Additionally, when inhaled for 5 days (5 h/day, 100 µg/m<sup>3</sup>), vanadium significantly increased Fe level in bronchial alveolar lavage fluid, indicating a redox effect. Our body has various anti-oxidant proteins which have the capacity to bind both endogenous and exogenous heavy metals, and these proteins, such as metallothionein, heme oxygenase-1, iron-binding proteins, nuclear factor erythroid like-2, glutathione S-transferase, and superoxide dismutase, can control oxidative stress through multiple pathways including inactivation of reactive oxygen species, scavenging free

radicals, chelation of prooxidative transition metals, and reduction of hydroperoxidase, and redox reaction-related elements play an important role in this process (Blanco-Ayala et al., 2014; Elias et al., 2008). Furthermore, increasing evidence has also shown that metal ions dissolved from metal oxide NPs can influence homeostasis of electrolytes in tissues via extensive mechanisms such as ion transporters, ion channels, redox reaction, and tubular reabsorption (Bal et al., 2013; Dubyak, 2004; Fowler et al., 1987; Goyer, 1997; Marchetti, 2014; Mondal et al., 2010; Valko et al., 2005). Notably, we found that tissue homeostasis of redox-response related elements was more clearly altered in the heart than in kidney and spleen which show high distribution unlike our expectation. Additionally, tissue levels of  $\text{Na}^+$  and  $\text{K}^+$  were remarkably elevated in the heart of mice exposed to  $\text{S-V}_2\text{O}_5$  and  $\text{S-V}_2\text{O}_3$  NPs and in the kidney of mice exposed to  $\text{S-V}_2\text{O}_3$  NPs,  $\text{Ca}^{2+}$  level was also clearly altered in tissues of mice exposed to all of VO NPs. Moreover, we observed that tissue accumulation of  $\text{V}_2\text{O}_5$  NPs was higher than that of  $\text{V}_2\text{O}_3$  and  $\text{VO}_2$  NPs, and in case of the same oxidation state, accumulation of S-VO NPs was higher compared to that of C-VO NPs. Therefore, we hypothesize that dissolution rates may play a key role in determining the biological effects of VO NPs evaluated in this study. Considering that the size of C-VO NPs was irregular, we also suggest that size (surface area) may be an important factor determining the biological effects of VO NPs. Moreover, we feel that further study is needed to elucidate specific effects of VO NPs on heart function (Shattock et al., 2015; Yang et al., 2015).

According to previous studies, exposure to vanadium can directly or indirectly influence the function of the host immune system (Cohen et al., 2007; Keil et al., 2016; Kulkarni et al., 2014; Pinon-Zarate et al., 2008). As mentioned previously, we could also observe VO NPs in both the blood and the spleen on 12 h after dosing with VO NPs. As well, C- and  $\text{S-V}_2\text{O}_5$  NPs remarkably accumulated in the spleen after dosing with VO NPs for 28 days. More interestingly, at the higher dose (210  $\mu\text{g}/\text{mouse}$ ), the number of WBC decreased in mice exposed to all the five types of VO NPs, and the levels of total protein and albumin were reduced in exposure to  $\text{S-V}_2\text{O}_5$  and  $\text{S-V}_2\text{O}_3$  NPs. While maturation of dendritic cells, a representative APC, was not influenced by exposure to VO NPs, except  $\text{S-V}_2\text{O}_5$  NPs, co-expression of CD80 and CD86, antigen presentation-related proteins, was significantly attenuated on the spleen following exposure to VO NPs, except C-VO<sub>2</sub> NPs. These data demonstrate that exposure to VO NPs may impair the immune function and metabolism regulation. In addition, RBC develops in the bone marrow and make up 40–45% of whole blood volume. Mature RBC is non-nucleated cell which cannot divide and has limited lifetime. Membrane of defective or worn-out RBC is changed making it susceptible to selective recognition by macrophages and undergoes subsequent phagocytic process by macrophages in spleen, liver and lymph node. RBC is finally mechanically filtrated in red pulp of the spleen, and their components are recycled by macrophages. Additionally, RBC can directly or indirectly influence cardiovascular function and immune response as well oxygen delivery (Barker et al., 2007; Hjelmt et al., 2006; Kor et al., 2009; Morera and MacKenzie, 2011; Ndungu et al., 2005; Urban et al., 1999). In this study, both  $\text{V}_2\text{O}_5$  NPs penetrated into the RBC and the maturation of dendritic cells was inhibited in mice exposed to  $\text{S-V}_2\text{O}_5$  NPs only. Considering that the maturation of dendritic cells can be modulated by RBC infected to malaria (Buttari et al., 2012; Elliott et al., 2007; Urban et al., 1999), we suggest the need of further study on toxic effects of NPs to RBC. Moreover, considering that the population of T cells was more dominated compared to that of B cells in the VO NP-treated groups, we hypothesize that the decreased expression of co-expression of CD80 and CD86 on the splenocytes may be at least partially attributed to the relative decrease in the population of APCs in the splenocytes.

In conclusion, we suggest that the biodistribution and toxic effects of VO NPs depends on dissolution and partially particle size (surface area). Further study is needed to elucidate specific effects on heart function and the immune system.

## Conflict of interest

The authors report no conflicts of interest to declare.

## Acknowledgement

This work was supported by the Basic Science Research Program, through the National Research Foundation of Korea, funded by the Ministry of Education, Science and Technology (2011-35B-E00011, 2016R1A2B2012728).

## Appendix A. Supplementary material

Supplementary data associated with this article can be found in the online version at <http://dx.doi.org/10.1016/j.envres.2016.05.036>.

## References

- Agency for toxic substances and disease registry (ATSDR), 2012. Toxicological profile for Vanadium. ([www.atsdr.cdc.gov/toxprofiles/tp58.pdf](http://www.atsdr.cdc.gov/toxprofiles/tp58.pdf)).
- Allianz AG and the Organisation for Economic Co-Operation and Development, 2005. Small Sizes That Matter: Opportunities and Risks of Nanotechnologies. At: ([www.oecd.org/science/nanosafety/37770473.pdf](http://www.oecd.org/science/nanosafety/37770473.pdf)), (accessed 22.05.15).
- Aust, A.E., Cook, P.M., Dodson, R.F., 2011. Morphological and chemical mechanisms of elongated mineral particle toxicities. *J. Toxicol. Environ. Health B: Crit. Rev.* 14 (1–4), 40–75.
- Bahlawane, N., Lenoble, D., 2014. Vanadium oxide compounds: structure, properties, and growth from the gas phase. *Chem. Vap. Depos.* 20 (7–9), 299–311.
- Bal, W., Sokolowska, M., Kurowska, E., Faller, P., 2013. Binding of transition metal ions to albumin: sites, affinities and rates. *Biochim. Biophys. Acta* 1830 (12), 5444–5455.
- Barker, R.N., Vickers, M.A., Ward, F.J., 2007. Controlling autoimmunity—lessons from the study of red blood cells as model antigens. *Immunol. Lett.* 108 (1), 20–26.
- Barros, L.F., Castro, J., Bittner, C.X., 2002. Ion Movements in cell death: from protection to execution. *Biol. Res.* 35 (2), 209–214.
- Basu, R., Harris, M., Sie, L., Malig, B., Broadwin, R., Green, R., 2014. Effects of fine particulate matter and its constituents on low birth weight among full-term infants in California. *Environ. Res.* 128, 42–51.
- Bell, M.L., Ebisu, K., Leaderer, B.P., Gent, J.F., Lee, H.J., Koutrakis, P., Wang, Y., Dominici, F., Peng, R.D., 2014. Associations of PM<sub>2.5</sub> constituents and sources with hospital admissions: analysis of four counties in Connecticut and Massachusetts (USA) for persons *ersons*Connecticut and Mass. *Health Perspect.* 122 (2), 138–144.
- Beyersmann, D., Hartwig, A., 2008. Carcinogenic metal compounds: recent insight into molecular and cellular mechanisms. *Arch. Toxicol.* 82 (8), 493–512.
- Bishayee, A., Chatterjee, M., 1993. Selective enhancement of glutathione S-transferase activity in liver and extrahepatitic tissues of rat following oral administration of vanadate. *Acta Physiol. Pharmacol. Bulg.* 19 (3), 83–89.
- Blanco-Ayala, T., Andérica-Romero, A.C., Pedraza-Chaverri, J., 2014. New insights into antioxidant strategies against paraquat toxicity. *Free Radic. Res.* 48 (6), 623–640.
- Bock, D.C., Takeuchi, K.J., Marschilok, A.C., Takeuchi, E.S., 2013. Silver vanadium oxide and silver vanadium phosphorous oxide dissolution kinetics: a mechanistic study with possible impact on future ICD battery lifetimes. *Dalton Trans.* 42 (38), 13981–13989.
- Borm, P., Klaessig, F.C., Landry, T.D., Moudgil, B., Pauluhn, J., Thomas, K., Trottier, R., Wood, S., 2006. Research strategies for safety evaluation of nanomaterials, (part V): role of dissolution in biological fate and effects of nanoscale particles. *Toxicol. Sci.* 90 (1), 23–32.
- Bruyère, V.I.E., Morando, P.J., Blesa, M.A., 1999. The dissolution of vanadium pentoxide in aqueous solutions of oxalic and mineral acids. *J. Colloid Interface Sci.* 209 (1), 207–214.
- Buttari, B., Profumo, E., Cuccu, B., Straface, E., Gambardella, L., Malorni, W., Genuini, I., Capoano, R., Salyati, B., Riganò, R., 2012. *Int. J. Cardiol.* 155 (3), 484–486.
- Chen, X., Wang, X., Wang, Z., Wan, J., Liu, J., Qian, Y., 2004. An ethylene glycol reduction approach to metastable  $\text{VO}_2$  nanowire arrays. *Nanotechnology* 15 (11), 1685.

- Cho, W.S., Kang, B.C., Lee, J.K., Jeong, J., Che, J.H., Seok, S.H., 2013. Comparative absorption, distribution, and excretion of titanium dioxide and zinc oxide nanoparticles after repeated oral administration. *Part. Fibre Toxicol.* 10, 9.
- Cohen, M.D., Sisco, M., Prophete, C., Chen, L.C., Zelikoff, J.T., Ghio, A.J., Stonehauer, J.D., Smeel, J.J., Holder, A.A., Crans, D.C., 2007. Pulmonary immunotoxic potentials of metals are governed by select physicochemical properties: vanadium agents. *J. Immunotoxicol.* 4 (1), 49–60.
- Domingo, J.L., 1996. Vanadium: a review of the reproductive and developmental toxicity. *Reprod. Toxicol.* 10 (3), 175–182.
- Domingo, J.L., Gomez, M., Llobet, J.M., Corbella, J., Keen, C.L., 1991. Oral vanadium administration to streptozotocin-diabetic rats has marked negative side-effects which are independent of the form of vanadium used. *Toxicology* 66 (3), 279–287.
- Dubyak, G.R., 2004. Ion homeostasis, channels, and transporters: an update on cellular mechanisms. *Adv. Physiol. Educ.* 28 (1–4), 143–154.
- Duffus, J.H., 2007. Carcinogenicity classification of vanadium pentoxide and inorganic vanadium compounds, the NTP study of carcinogenicity of inhaled vanadium pentoxide, and vanadium chemistry. *Regul. Toxicol. Pharmacol.* 47 (1), 110–114.
- Ehrlich, V.A., Nersesyan, A.K., Atefie, K., Hoelzl, C., Ferk, F., Bichler, J., Valic, E., Schaffer, A., Schulte-Hermann, R., Fenech, M., Wagner, K.H., Knasmüller, S., 2008. Inhalative exposure to vanadium pentoxide causes DNA damage in workers: results of a multiple end point study. *Environ. Health Perspect.* 116 (12), 1689–1693.
- Elias, R.J., Kellerby, S.S., Decker, E.A., 2008. Antioxidant activity of proteins and peptides. *Crit. Rev. Food Sci. Nutr.* 48 (5), 430–441.
- Elliott, S.R., Spurck, T.P., Dodin, J.M., Maier, A.G., Voss, T.S., Yosaatmadja, F., Payne, P.D., McFadden, G.I., Cowman, A.F., Rogerson, S.J., Schofield, L., Brown, G.V., 2007. Inhibition of dendritic cell maturation by malaria is dose dependent and does not require Plasmodium falciparum erythrocyte membrane protein 1. *Infect. Immun.* 75 (7), 3621–3632.
- Fickl, H., Theron, A.J., Grimmer, H., Oomen, J., Ramafi, G.J., Steel, H.C., Visser, S.S., Anderson, R., 2006. Vanadium promotes hydroxyl radical formation by activated human neutrophils. *Free Radic. Biol. Med.* 40 (1), 146–155.
- Fowler, B.A., Goering, P.L., Squibb, K.S., 1987. Mechanism of cadmium-methallothionein-induced nephrotoxicity: relationship to altered renal calcium metabolism. *Exp. Suppl.* 52, 661–668.
- Goyer, R.A., 1997. Toxic and essential metal interactions. *Annu. Rev. Nutr.* 17, 37–50.
- Ha, D., Joo, H., Ahn, G., Kim, M.J., Bing, S.J., An, S., Kim, H., Kang, K.G., Lim, Y.K., Lee, Y., 2012. Jeju ground water containing vanadium induced immune activation on splenocytes of low dose  $\gamma$ -rays-irradiated mice. *Food Chem. Toxicol.* 50 (6), 2097–2105.
- Hjelm, F., Carlsson, F., Getahun, A., Heyman, B., 2006. Antibody-mediated regulation of the immune response. *Scand. J. Immunol.* 64 (3), 177–184.
- Holmes, A.M., Song, Z., Moghimi, H.R., Roerts, M.S., 2016. Relative penetration of zinc oxide and zinc ions into human skin after application of different zinc oxide formulations. *ACS Nano* 10 (2), 1810–1819.
- International Agency for Research on Cancer (IARC), 2006. IARC Monographs on the evaluation of Carcinogenic Risks to humans. Volume 86. Cobalt in Hard Metals and Cobalt Sulfate, Gallium Arsenide, Indium Phosphide and Vanadium pentoxide. <http://monographs.iarc.fr/ENG/Monographs/vol86/>.
- Imtiaz, M., Rizwan, M.S., Xiong, S., Li, H., Ashraf, M., Shahzad, S.M., Shahzad, M., Rizwan, M., Tu, S., 2015. Vanadium, recent advancements and research prospects: a review. *Environ. Int.* 80, 79–88.
- Ivask, A., Juganson, K., Bondarenko, O., Mortimer, M., Aruoja, V., Kasemets, K., Blinova, I., Heinlaan, M., Slaveyko, V., Kahru, A., 2014. Mechanisms of toxic action of Ag, ZnO and CuO nanoparticles to selected ecotoxicological test organisms and mammalian cells in vitro: a comparative review. *Nanotoxicology* 8 (Suppl. 1), S57–S71.
- Kang, Y.B., 2012. Critical evalution and thermodynamic optimization of the VO-VO<sub>2.5</sub> system. *J. Eur. Ceram. Soc.* 32 (12), 3187–3198.
- Keil, D., Buck, B., Goossens, D., Teng, Y., Leetham, M., Murphy, L., Pollard, J., Eggers, M., McLaurin, B., Gerads, R., DeWitt, J., 2016. Immunotoxicological and neurotoxicological profile of health effects following subacute exposure to geogenic dust from sand dunes at the Nellis Dunes Recreation Area, Las Vegas, NV. *Toxicol. Appl. Pharmacol.* 291, 1–12.
- Kim, J.Y., Hauser, R., Wand, M.P., Herrick, R.F., Amarasiwardena, C.J., Christiani, D.C., 2003. The association of expired nitric oxide with occupational particulate metal exposure. *Environ. Res.* 93 (2), 158–166.
- Kor, D.J., Van Buskirk, C.M., Gajic, O., 2009. Red blood cell storage lesion. *Bosn. J. Basic Med. Sci.* 9 (Suppl. 1), S21–S27.
- Krośniak, M., Francik, R., Kowalska, J., Grybos, R., Bluz, M., Kwiatek, W.M., 2013. Effects of vanadium complexes supplementation on V, Fe, Cu, Zn, Mn, Ca and K concentration in STZ diabetic rat's spleen. *Acta Pol. Pharm.* 70 (1), 71–77.
- Kulkarni, A., Kumar, G.S., Kaur, J., Tikoo, K., 2014. A comparative study of the toxicological aspects of vanadium pentoxide and vanadium oxide nanoparticles. *Inhal. Toxicol.* 26 (13), 772–788.
- Langeroodi, N.S., 2012. Silica-supported vanadium oxide nanoparticles as efficient heterogeneous catalyst for hydrolysis of sucrose. *Russ. J. Phys. Chem. A* 86 (4), 628–631.
- Larsson, M.A., Baken, S., Smolders, E., Cubadda, F., Gustafsson, J.P., 2015. Vanadium bioavailability in soils amended with blast furnace slag. *J. Hazard. Mater.* 296, 158–165.
- Magari, S.R., Schwartz, J., Williams, P.L., Hauser, R., Smith, T.J., Christiani, D.C., 2002. The association of particulate air metal concentrations with heart rate variability. *Environ. Health Perspect.* 110 (9), 875–880.
- Marchetti, C., 2014. Interaction of metal ions with neurotransmitter receptors and potential role in neurodiseases. *Biometals* 27 (6), 1097–1113.
- Mondal, S., Haldar, S., Saha, P., Ghosh, T.K., 2010. Metabolism and tissue distribution of trace elements in broiler chickens' fed diets containing deficient and plethoric levels of copper, manganese, and zinc. *Biol. Trace Elem. Res.* 137 (2), 190–205.
- Morera, D., MacKenzie, S.A., 2011. Is there a direct role for erythrocytes in the immune response? *Vet. Res.* 42, 89.
- National Nanotechnology Initiative (NNI), 2014. Supplement to the President's FY 2015 Budget.
- Ndungu, F.M., Urban, B.C., Marsh, K., Langhorne, J., 2005. Regulation of immune response by plasmodium-infected red blood cells. *Parasite Immunol.* 27 (10–11), 373–384.
- Ng, S.H., Patey, T.J., Büchel, R., Krumeich, F., Wang, J.Z., Liu, H.K., Pratsinis, S.E., Novák, P., 2009. Flame spray-pyrolyzed vanadium oxide nanoparticles for lithium battery cathodes. *Phys. Chem. Chem. Phys.* 11 (19), 3748–3755.
- Övey, I.S., Naziroğlu, M., 2015. Homocysteine and cytosolic GSH depletion induce apoptosis and oxidative toxicity through cytosolic calcium overload in the hippocampus of aged mice: involvement of TRPM2 and TRPV1 channels. *Neuroscience* 284, 225–233.
- Park, E.J., Oh, S.Y., Lee, S.J., Lee, K., Kim, Y., Lee, B.S., Kim, J.S., 2015. Chronic pulmonary accumulation of iron oxide nanoparticles induced Th1-type immune response stimulating the function of antigen-presenting cells. *Environ. Res.* 143 (Pt A), 138–147.
- Pinon-Zarate, G., Rodriguez-Lara, V., Rojas-Lemus, M., Martinez-Pedraza, M., Gonzalez-Villalva, A., Mussali-Galante, P., Fortoul, T.I., Barquet, A., Masso, F., Montano, L.F., 2008. Vanadium pentoxide inhalation provokes germinal center hyperplasia and suppressed humoral immune responses. *J. Immunotoxicol.* 5 (2), 115–122.
- Rampelberg, G., Schutter, B.D., Devulder, W., Martens, K., Radub, I., Detavernier, C., 2015. In situ x-ray diffraction study of the controlled oxidation and reduction in the V-O system for the synthesis of VO<sub>2</sub> and V<sub>2</sub>O<sub>3</sub> thin films. *J. Mater. Chem. C* 3 (43), 11357–11365.
- Restrepo-Angulo, I., De Vizcaya-Ruiz, A., Camacho, J., 2010. Ion channels in toxicology. *J. Appl. Toxicol.* 30 (6), 497–512.
- Reul, B.A., Amin, S.S., Buchet, J.P., Ongembra, L.N., Crans, D.C., Brichard, S.M., 1999. Effects of vanadium complexes with organic ligands on glucose metabolism: a comparison study in diabetic rats. *Br. J. Pharmacol.* 126 (2), 467–477.
- Rhoads, L.S., Silkworth, W.T., Roppolo, M.L., Whittingham, M.S., 2010. Cytotoxicity of nanostructured vanadium oxide on human cells in vitro. *Toxicol. Vitr.* 24 (1), 292–296.
- Sabella, S., Carney, R.P., Brunetti, V., Malvindi, M.A., Al-Juffali, N., Vecchio, G., James, S.M., Bakr, O.M., Cingolani, R., Stellacci, F., Pompa, P.P., 2014. A general mechanism for intracellular toxicity of metal-containing nanoparticles. *Nanoscale* 6 (12), 7052–7061.
- Santulli, G., Xie, W., Reiken, S.R., Marks, A.R., 2015. Mitochondrial calcium overload is a key determinant in heart failure. *Proc. Natl. Acad. Sci. USA* 112 (36), 11389–11394.
- Shattock, M.J., Ottolia, M., Bers, D.M., Blaustein, M.P., Boguslavskyi, A., Bossuyt, J., Bridge, J.H., Chen-Izu, Y., Clancy, C.E., Edwards, A., Goldhaber, J., Kaplan, J., Lingrel, J.B., Pavlovic, D., Philipson, K., Sipido, K.R., Xie, Z.J., 2015. Na<sup>+</sup>/Ca<sup>2+</sup> exchange and Na<sup>+</sup>/K<sup>+</sup>-ATPase in the heart. *J. Physiol.* 593 (6), 1361–1382.
- Shidong, J., Feng, Z., Ping, J., 2011. Preparation of high performance pure single phase VO<sub>2</sub> nanopowder by hydrothermally reducing the V<sub>2</sub>O<sub>5</sub> gel. *Sol. Energy Mat. Sol. Cells* 95 (12), 3520–3526.
- Takeo, S., Tanonaka, K., 2004. Na<sup>+</sup> overload-induced mitochondrial damage in the ischemic heart. *Can. J. Physiol. Pharmacol.* 82 (12), 1033–1043.
- Thompson, K.H., 1999. Vanadium and diabetes. *Biofactors* 10 (1), 43–51.
- Tsang, C., Manthiram, A., 1997. Synthesis of nanocrystalline VO<sub>2</sub> and its electrochemical behavior in lithium batteries. *J. Electrochem. Soc.* 144 (2), 520–524.
- Urban, B.C., Ferguson, D.J., Pain, A., Willcox, N., Plebanski, M., Austyn, J.M., Roberts, D.J., 1999. Plasmodium falciparum-infected erythrocytes modulate the maturation of dendritic cells. *Nature* 400 (6739), 73–77.
- Ustarroz-Cano, M., García-Peláz, I., Piñón-Zárate, G., Herrera-Enríquez, M., Soldevila, G., Fortoul, T.I., 2012. CD11c decrease in mouse thymic dendritic cells after vanadium inhalation. *J. Immunotoxicol.* 9 (4), 374–380.
- Utembe, W., Potgieter, K., Stefaniak, A.B., Gulumian, M., 2015. Dissolution and biodegradability: important parameters needed for risk assessment of nanoparticles. *Part. Fibre Toxicol.* 12, 11.
- Valko, M., Morris, H., Cronin, M.T., 2005. Metals, toxicity and oxidative stress. *Curr. Med. Chem.* 12 (10), 1161–1208.
- Wang, D., Lin, Z., Wang, T., Yao, Z., Qin, M., Zheng, S., Lu, W., 2016. Where does the toxicity of metal oxide nanoparticles come from: the nanoparticles, the ions, or a combination of both? *J. Hazard. Mater.* 308, 328–334.
- Wiecinski, P.N., Metz, K.M., Mangham, A.N., Jacobson, K.H., Hamers, R.J., Pedersen, J.A., 2009. Gastrointestinal biodegradability of engineered nanoparticles: development of an in vitro assay. *Nanotoxicology* 3 (3), 202–214.
- World Health Organization (WHO), 2001. Vanadium pentoxide and Other Inorganic Vanadium Compounds. [www.who.int/ipcs/publications/cicad/en/cicad29.pdf](http://www.who.int/ipcs/publications/cicad/en/cicad29.pdf).
- Wörle-Knirsch, J.M., Kern, K., Schlech, C., Adelhelm, C., Feldmann, C., Krug, H.F., 2007. Nanoparticulate vanadium oxide potentiated vanadium toxicity in human lung cells. *Environ. Sci. Technol.* 41 (1), 331–336.
- Yang, K.C., Kyle, J.W., Makielski, J.C., Dudley Jr., S.C., 2015. Mechanisms of sudden cardiac death: oxidants and metabolism. *Circ. Res.* 116 (12), 1937–1955.
- Zhang, C., Hu, Z., Deng, B., 2016. Silver nanoparticles in aquatic environments: physicochemical behavior and antimicrobial mechanisms. *Water Res.* 88, 403–427.

- Zhang, H., Ji, Z., Xia, T., Meng, H., Low-Kam, C., Liu, R., Pokhrel, S., Lin, S., Wang, X., Liao, Y.P., Wang, M., Li, L., Rallo, R., Damoiseaux, R., Telesca, D., Mädler, L., Cohen, Y., Zink, J.I., Nel, A.E., 2012. Use of metal oxide nanoparticle band gap to develop a predictive paradigm for oxidative stress and acute pulmonary inflammation. *ACS Nano* 6 (5), 4349–4368.
- Zhu, K., Qiu, H., Zhang, Y., Zhang, D., Chen, G., Wei, Y., 2015. Synergetic effects of  $\text{Al}^{3+}$  doping and grapheme modification on the electrochemical performance of  $\text{V}_2\text{O}_5$  cathode materials. *ChemSusChem* 8 (6), 1017–1025.